

LAB DEMONSTRATION OF INTERFEROMETRIC MEASUREMENT USING A TEST PLATE AND CGH

Presented to:

Larry Stepp
Eric Hansen

The Association of Universities for Research in Astronomy, Inc.
Tucson, AZ, 85726

Prepared By

Feenix Y. Pan
Jim H. Burge

Optical Science Center
University of Arizona
Tucson, AZ 85747

Dave Anderson
Rayleigh Optical Corp.

06/2002

Contents

EXECUTIVE summary	3
1. Theory of Operation.....	4
2. Optical configuration	6
3. Experimental Results.....	11
4. Error Analysis	12
5. How to improve the test	13
5.1 Co-axial setup reduces the slope requirement for the test plate.....	13
5.2 Method to ease the projection system requirement.....	15
5.3 Making the test cost effective and less complex.....	16
Conclusion.....	17

EXECUTIVE SUMMARY

This report presents results from a contracted study on experimental validation of a new method for measuring off-axis aspheric segments by utilizing a small computer generated hologram (CGH) and a full aperture test plate. This report briefly revisits the theory of operation (section 1.0) and details the laboratory optical configuration for the experiment (section 2.0). Results from the experiment are detailed in section 3, followed by section 4.0 in which a detailed error analysis is included. Section 5 illustrates two insights on how to make the test more cost effective and less complex. Preliminary analysis indicates that this new method has full potential for providing high measurement accuracy at a low cost and greatly reducing the individual segment measure time.

1. THEORY OF OPERATION

The proposed test is a null test. In this test, the concave segment is compared to the convex spherical reference surface of the test plate. CGHs are used to compensate for any aspherical departure of the segment from the spherical reference surface. The test plate reference surface is chosen to be spherical, since compared to aspherical surfaces, spherical surfaces are more cost effectively manufactured to high accuracy. Figure 1-1 illustrates how a CGH combined with a test plate is used to measure off-axis aspherical segments:

- A Laser beam is first expanded to uniformly illuminate the CGH.
- The CGH is imaged onto the test surface by the projection lens
- Two CGH diffraction orders, 0th and 1st, are selected by placing the object stop at the focal plane of the projection lens.
- The reference beam has a spherical wavefront. It originates from the 0th diffraction order of the CGH, reflects off the reference side of the test plate, and then reaches the charge-coupled device (CCD).
- The test beam originates from the 1st order of the CGH. It has a pre-distorted wavefront that matches the shape of the aspherical mirror segment under test. After reflecting off the test surface, it too reaches the CCD.
- When the aspherical test surface perfectly matches the wavefront prescribed by the CGH, a null fringe is observed on the CCD. When this is not the case, fringes result. For added measurement accuracy, phase shifting interferometry (PSI) should be implemented by translating the segment under test via three piezo-electric transducers (PZTs).
- The image lens is chosen so that the test surface is imaged onto the CCD.
- The Image stop is placed at the front focal plane of the image lens to select appropriate orders (Figure 1-2 and Figure 1-3).

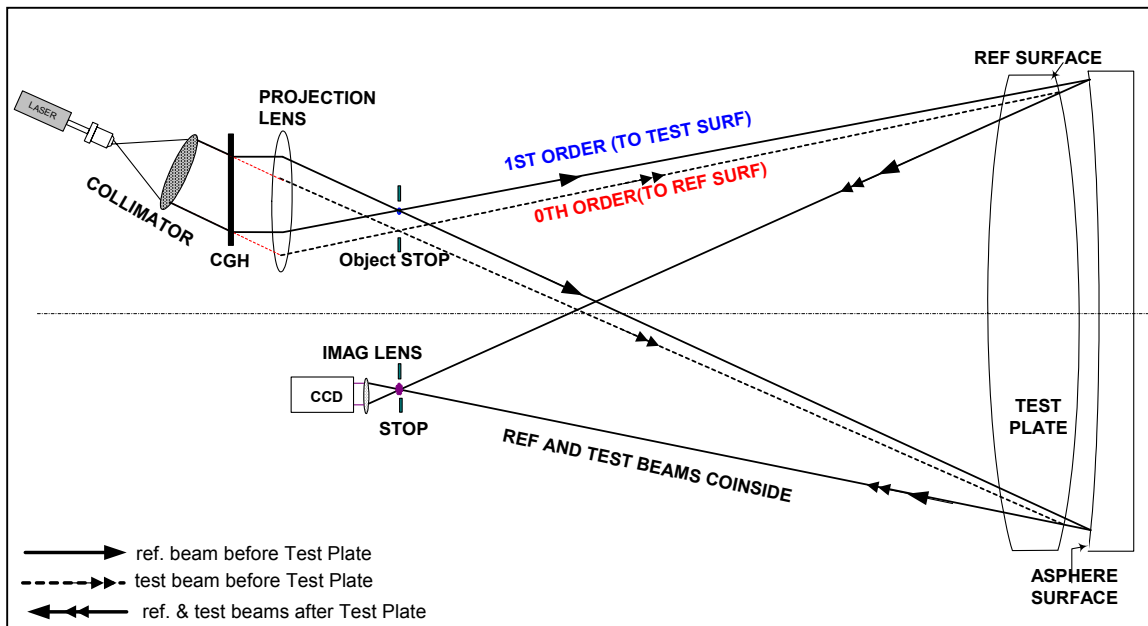


Figure 1-1 Theory of operation

Order from CGH	Reflected from	Final destination
Zero order	Test plate	Reference beam
	Segment	Blocked at the image stop
First order	Segment	Test beam
	Test plate	Blocked at image stop
All other orders	-----	Blocked at the stop following the projection lens

Figure 1-2 Order selections of the CGH test

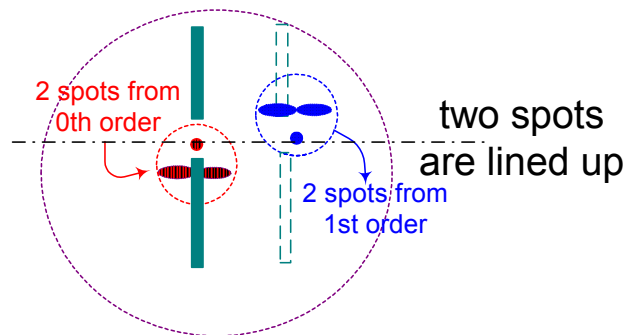


Figure 1-3: Selecting appropriate spots at the image stop for interference

This test is ideal for testing large quantities of off-axis aspherical segments. It produces excellent relative radii of curvatures (ROC) matching since, during the test, all concave aspheric segments are compared to the same convex spherical reference surface. It is also efficient since a single test setup can be optimized to accommodate measurement of all segments by simply replacing the CGH. In addition, this method is cost effective: 1) it ensures that both reference and test beams coincide at the CGH, so that the CGH can be written on a standard lithography substrate, and 2) it allows the test plate to be made from a non-precision transmission grade glass, like Zerodur. Finally, by employing PSI and utilizing its inherent near-common path configuration, this test achieves a high degree of measurement accuracy. Accurate axis location is achieved by implementing alignment marks on the CGH directly.

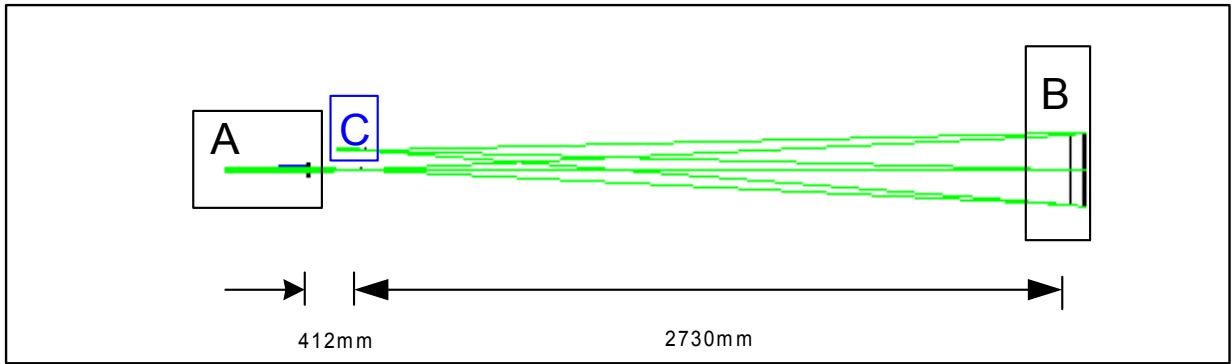
2. OPTICAL CONFIGURATION

The CGH testing method was demonstrated in a laboratory. A plano-convex test plate was used to measure a concave sphere of known surface quality. A computer-generated hologram was designed and used in the same manner as the asphere test, but the pattern corresponded to testing of a sphere. This changes very little in the test sensitivity, as a large tilt carrier always dominates the hologram and its sensitivity.

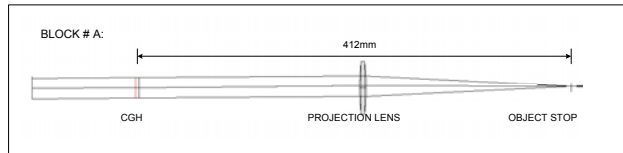
The system that we used to validate the computer models for the test design and the error analysis included the following:

- Matching 30 cm test plate and test sphere;
- A hologram of 20cm in diameter consist of chrome patterns written onto flat glass substrates;
- An off-the-shelf bi-convex lens with $F=200\text{mm}$ (as the projection system)
- An off-the-shelf plano-concave lens $F=50.2\text{mm}$ (as imaging system)

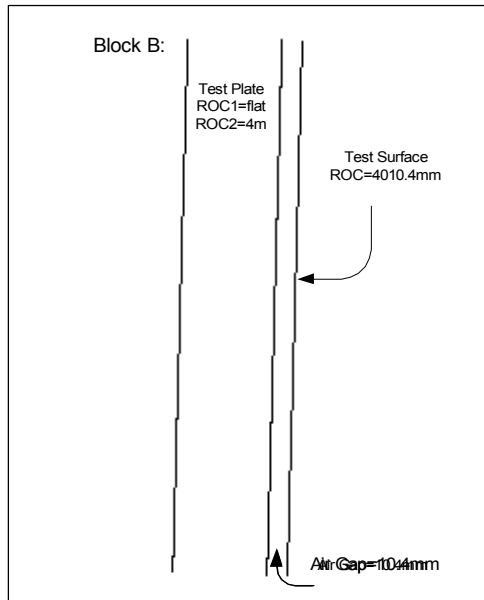
Phase shifting was done by translating the test sphere. And this movement is accomplished by positioning three PZTs on the back of the test surface. Figure 2-1 shows the schematics of the system, and Figures 2-2, 2-3 and 2-4 show the actual laboratory setup. A sample CGH used for the test is shown in Figure 2-5 (magnified 10x) and Table 2-1 shows the corresponding Zernike terms describing the CGH. A sample interferogram is shown in Figure 2-6 and corresponding phase map of the test surface is shown in Figure 2-7.



Details of
Block A



Details of
block B



Details of
block C

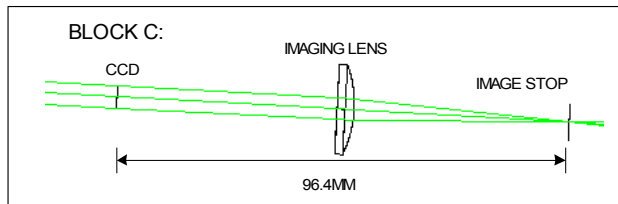


**Figure 2-1: schematics of the laboratory setup (to scale).
Blocks A, B and C are magnified**

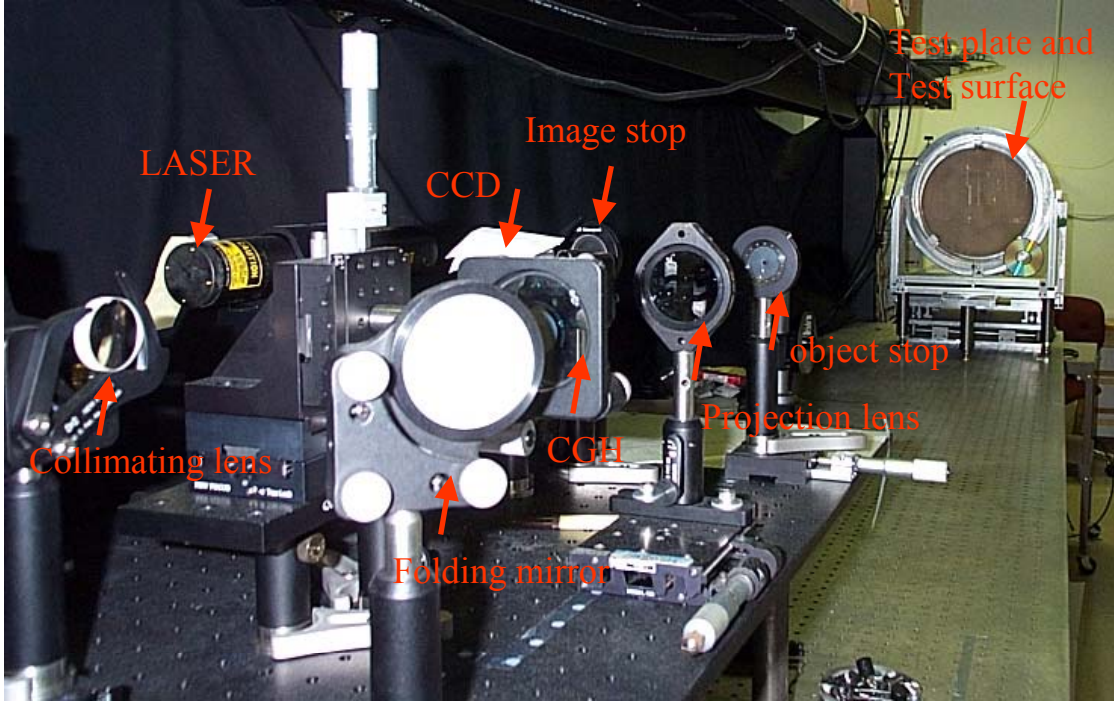


Figure 2-2: laboratory setup

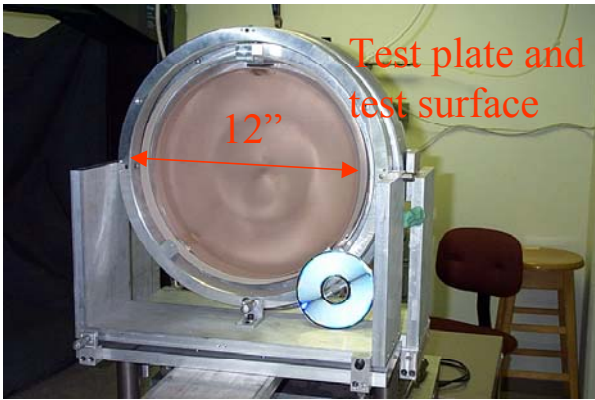


Figure 2-3 Test plate and test surface

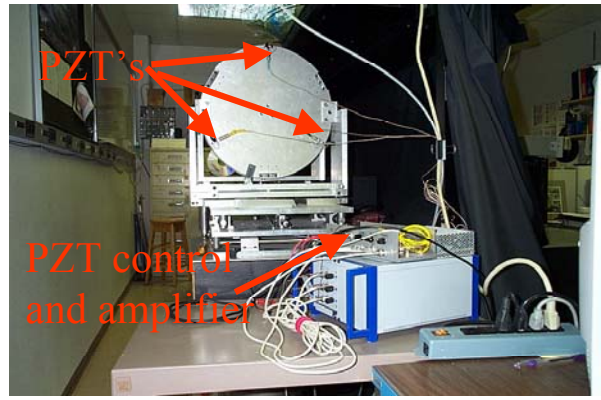


Figure 2-4 Back side of the test surface has 3 PZT's for

Number of terms:	37
Maximum rad ap :	35.2
Zernike Term 1:	0
Zernike Term 2:	-68.040908
Zernike Term 3:	-1574.8262
Zernike Term 4:	-24.72764
Zernike Term 5:	-152.4588
Zernike Term 6:	0.0073103072
Zernike Term 7:	-34.067373
Zernike Term 8:	-0.60370118
Zernike Term 9:	-1.3974876
Zernike Term 10:	0.18169425
Zernike Term 11:	0.01944716
Zernike Term 12:	-0.069184665
Zernike Term 13:	0.006296563
Zernike Term 14:	-0.027801011
Zernike Term 15:	0.056276342
Zernike Term 16:	0
Zernike Term 17:	-0.0004954872
Zernike Term 18:	-6.5925187e-005
Zernike Term 19:	-0.00077217093
Zernike Term 20:	-0.00022425369
Zernike Term 21:	0.0058559236
Zernike Term 22:	0
Zernike Term 23:	0.0026082074
Zernike Term 24:	0.0009272519
Zernike Term 25:	0.00014210407
Zernike Term 26:	0
Zernike Term 27:	0
Zernike Term 28:	-0.00062303239
Zernike Term 29:	0
Zernike Term 30:	-0.0004669993
Zernike Term 31:	0
Zernike Term 32:	0
Zernike Term 33:	0
Zernike Term 34:	0
Zernike Term 35:	0
Zernike Term 36:	0
Zernike Term 37:	0

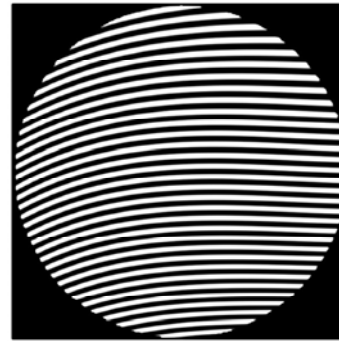


Figure 2-5: a sample CGH (magnified 10x)

Table 2-1: A sample CGH represented in 37 Zernike Terms

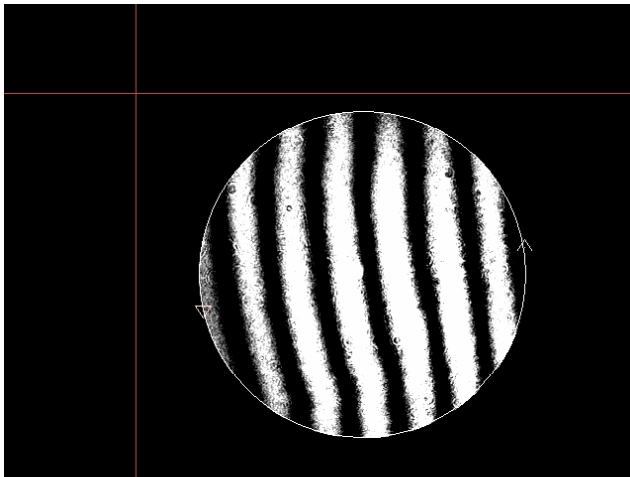


Figure 2-6: a sample interferogram

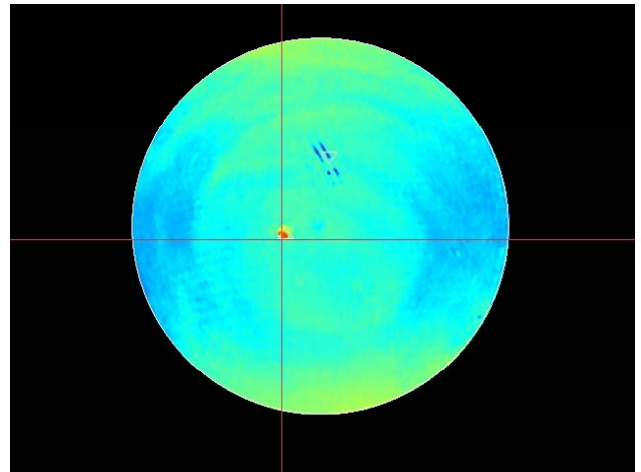
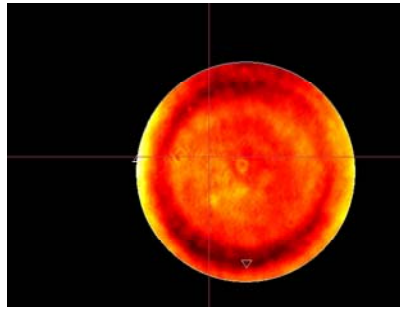


Figure 2-7: surface map of the test surface

3. EXPERIMENTAL RESULTS

One of the best ways to validate a new testing method is to compare measurements with a calibrated instrument. Figure 3-1 contains a surface plot of the test surface without CGH, and Figure 3-2 shows a surface measurement with CGH. Two measurements compare well: the RMS is less than 0.0171 waves, and with lower order aberration removed this number reduces to 0.0069 waves (3-3).



**Figure 3-1: Measurement result using proposed method
RMS=0.0369 waves**

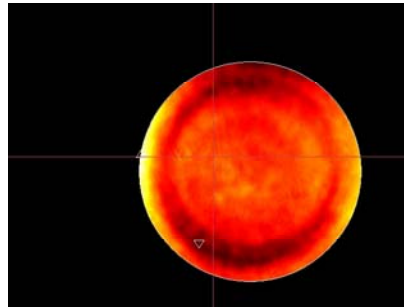


**Figure 3-2: Measurement result using traditional method
Rms=0.0490 waves**

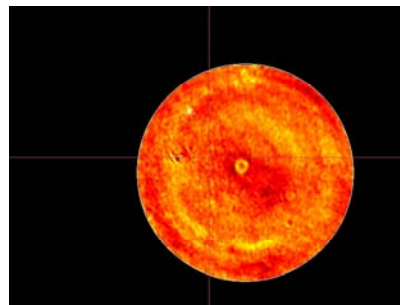


**Figure 3-3: Measurement differences
Rms=0.0079 waves**

4. ERROR ANALYSIS

Detailed error analysis was performed on the computer model of the system to obtain the theoretical accuracy of the test. Each error term is graphically shown in Figure 4-1. The two dominating error sources are projection lens and test plate non-reference side. From this analysis, we were able to arrive at two important conclusions on how to reduce system errors (section 5).

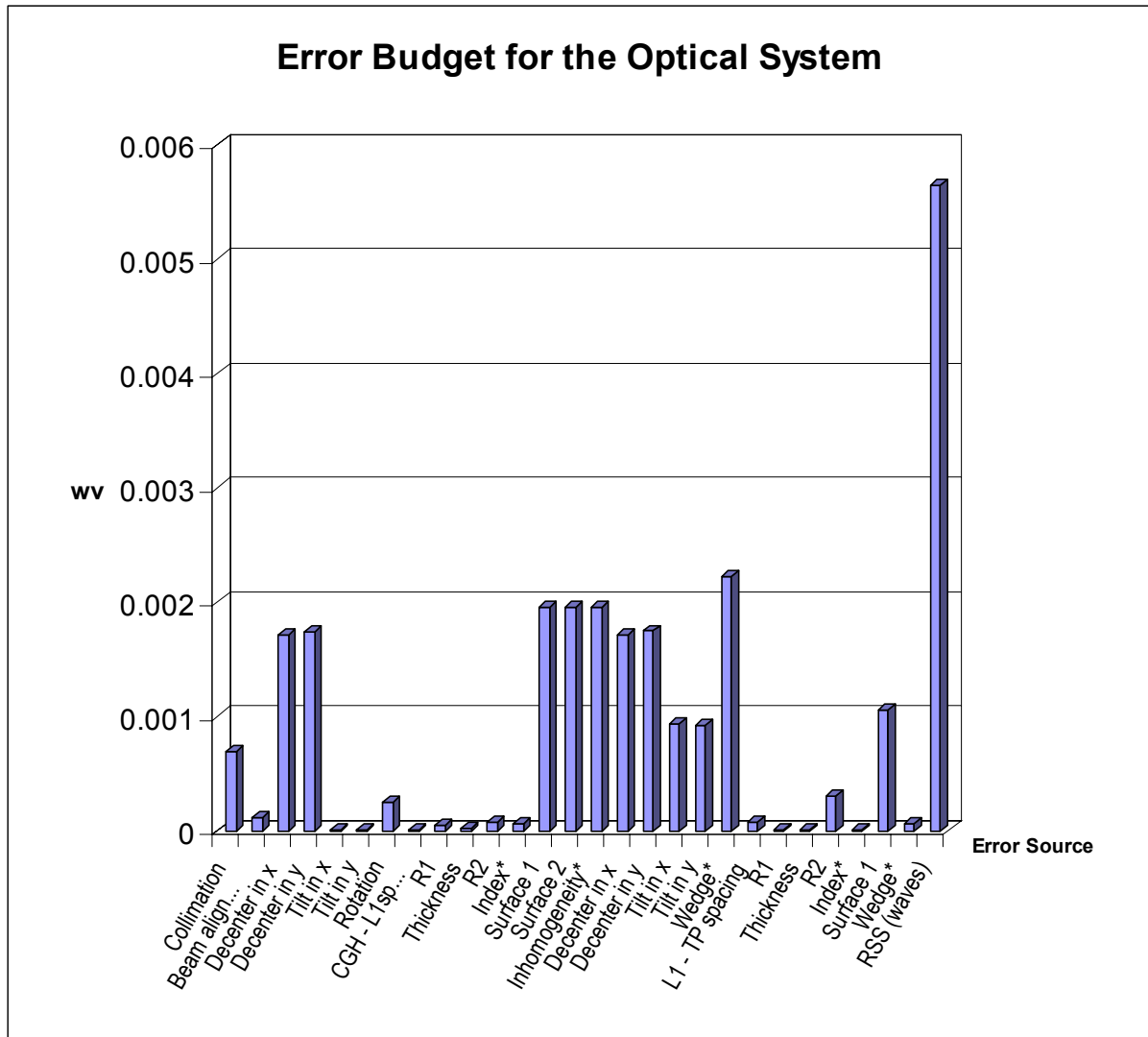


Figure 4-1: Error budget of the optical system

5. HOW TO IMPORVE THE TEST

Using the results obtained though the tolerance analysis in the previous section, this section draw two important conclusions on how to (a) make the test more cost effective (section 5.1), and (b) reduce the design complexity of the projection system (section 5.2).

5.1 Co-axial setup reduces the slope requirement for the test plate

At a first glance, it may seems like that the only way to reduce error caused by the non-reference side of test plate is to tighten its surface slope requirement. This can be costly. A closer examination, however, reveals that a more cost effective way to reduce this error is to have beams impinging onto and returning from the test plate co-axial (Figure 5-2). This is because, even though the reference beam and the test beam are nearly common path before reaching the test plate, they experience a small lateral shear at the test plate non-reference side (Figure 5-1). After recombination at the reference-side of the test plate, the reference and test beams are completely common path. This small lateral shear on the non-reference side leads to the error term associated with the test plate. Consider this numerical example:

In the test setup, the test plate is tilted $\alpha_{mechanical_tilt}$ of 1.6° with respect to the optical axis of the projection system, so that the imaging system can be spatially separated from the projection system. This 1.6° will cause reference and test beams to have a lateral shear of 910um on the non-reference side of the test plate. This shear leads to ~ 0.002 wv wavefront error assuming that the non-reference side of the test plate has surface slope of 0.02wv/cm and $n=1.458$ for Silica. This is calculated from $\Delta w = 2 \times (n - 1) \times \left(\frac{\Delta s}{\Delta x} \right) \times \Delta x$. (ZEMAX simulation confirms that $\Delta w = 0.003$ wv).

Instead of tightening the surface slope requirement, which is expensive, it is cost effective to reduce the amount of shear (Δx). This can be accomplished by having both entering and return beams off the test plate co-axial (Figure 5-2). Also by inserting a pellicle beam splitter, the projection system can be spatially separate from the image system. Figure 5-3 shows the dependence of shear (Δx) on mechanic tilt (angle α): as mechanical tilt angle α increases, shear Δx increases and leads to higher wavefront error. By using co-axial setup, shear between the reference and test beams can be limited to its

minimum: $\Delta x_{min} \approx \Delta t_{glass} \times \sin^{-1} \left(\frac{\epsilon_{max}}{n_{glass}} \right)$. For the case calculated above, this means Δx can be reduced from 910um to 14 um, thus reducing the wavefront error from 0.002 wv to 0.000013 wv.

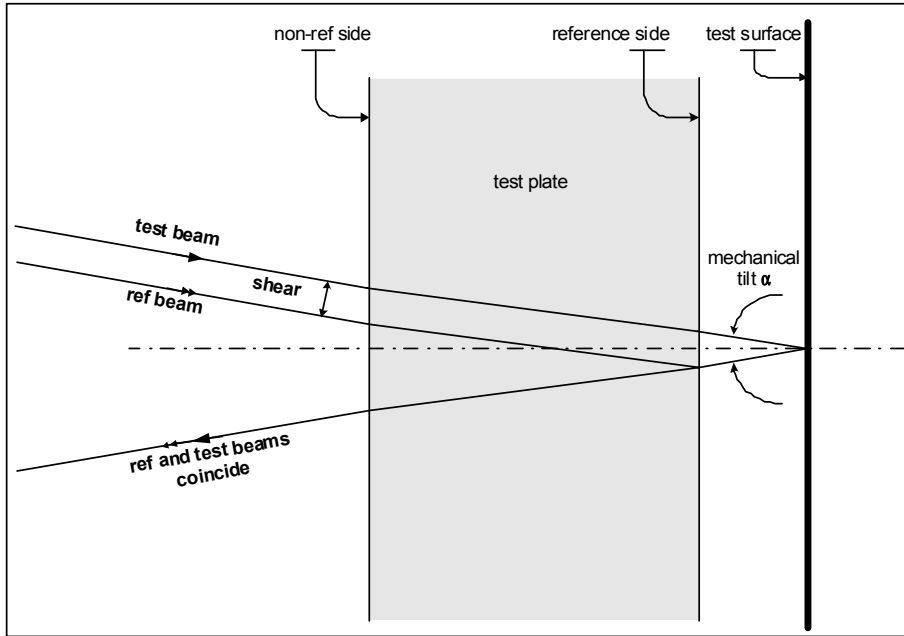


Figure 5-1: Non-coaxial setup increases the beam shears s at the illumination-side of test plate

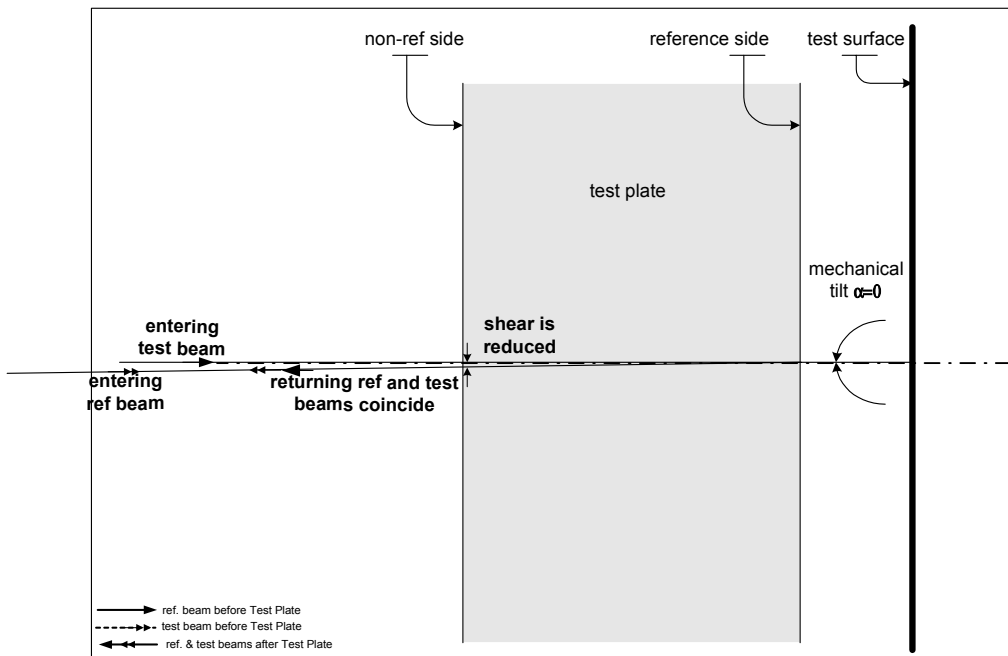


Figure 5-2: Co-axial setup reduces the beam shears s at the illumination-side of test plate

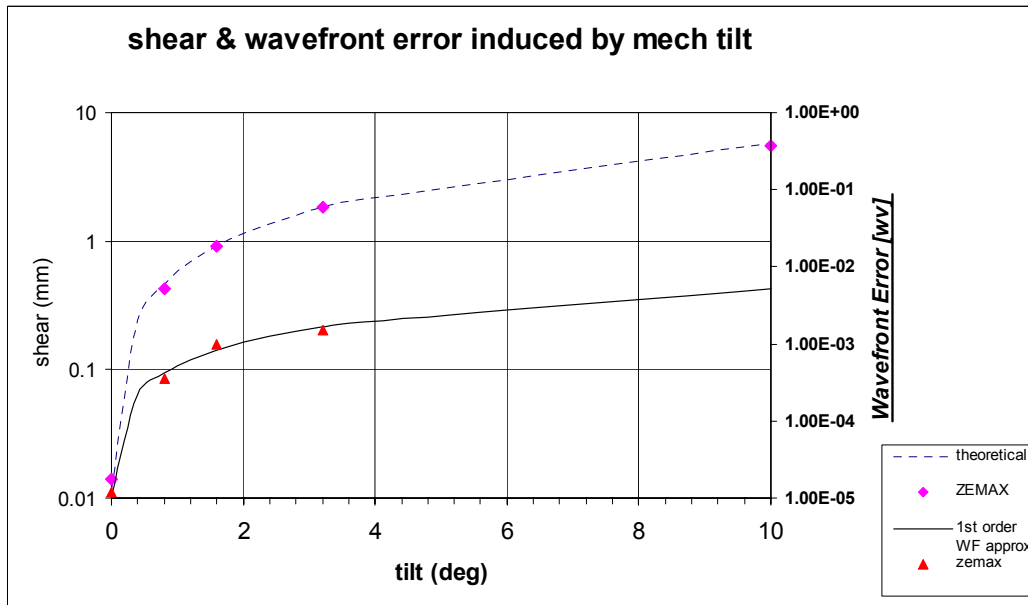


Figure 5-3: Shear and wavefront error linearly depend on the mechanical tilt angle

Using the finding discussed above, the system can be improved to be more cost effective by reducing the requirement on the surface slope of the test plate:

Use a pellicle beam splitter to spatially separate the image system from the projection system. This means that the surface slope of the test plate non-reference side can be

reduced from $\frac{0.02\lambda}{cm}$ to $\frac{1.6\lambda}{cm}$, yet still achieve accuracy of

$$\Delta w_{test_plate} = 2 \times (14\mu m) \times (n-1) \times \left(\frac{1.6\lambda}{cm} \right), \text{ or } 0.002wv.$$

5.2 Method to ease the projection system requirement

The projection system contributes to the overall system error and should be optimized to meet the error budget allocate to this error source. However, there is no advantage in perfecting the projection system beyond an “optimal point.” Beyond this point, the increase in cost outweighs the improvement in the system performance. One way to quantify this “optimal point” is by specifying the RMS wavefront error of the projection system. Consider this numerical example:

Suppose that total measurement accuracy needs to be 5nm RMS in surface measurement, which is equivalent to 10nm RMS in wavefront. Since there are three major contributing error sources as discussed earlier, each can be allocated approximately $10nm/\sqrt{3}$ or 5.77nm RMS wavefront error. Assuming that each of the two beams impinging upon the projection system picks up equal amount of RMS error (σ_{wv_error}) from the projection system, then $5.77nm = \sqrt{2 \times \sigma_{wv_error}}$. This then gives an upper bound on $\sigma_{wv_error} = 4.08nm$ or 0.0065 wv RMS in wavefront (or ~ 0.025 wv PV).

Another checkpoint of the “optimal point” is that the maximum transverse ray aberration, ϵ , of the projection system should be less than Δx_{\min} (14 μm for the case discussed above). This is to ensure that shear at the test plate is kept at its minimum so the surface slope requirement of the test plate need not to be tightened beyond what is necessary.

Having the 1st diffraction order of CGH centered on the projection system’s axis (Figure 5-4 and Figure 5-5) significantly reduces the size of the stop, and thus simplifies and ease the design of the projection system.

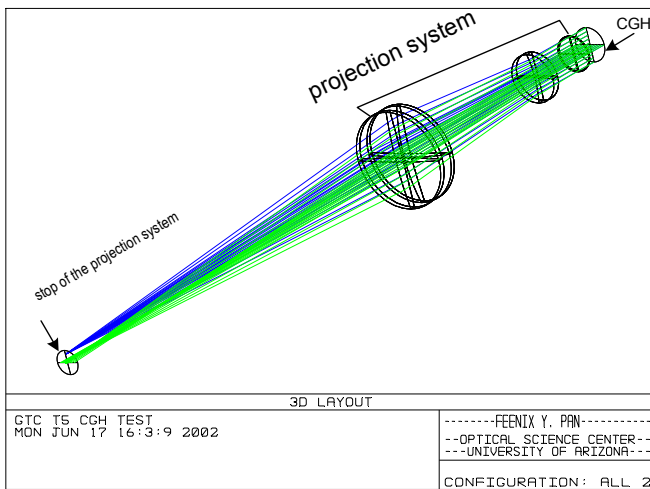


Figure 5-4: stop location of the projection system

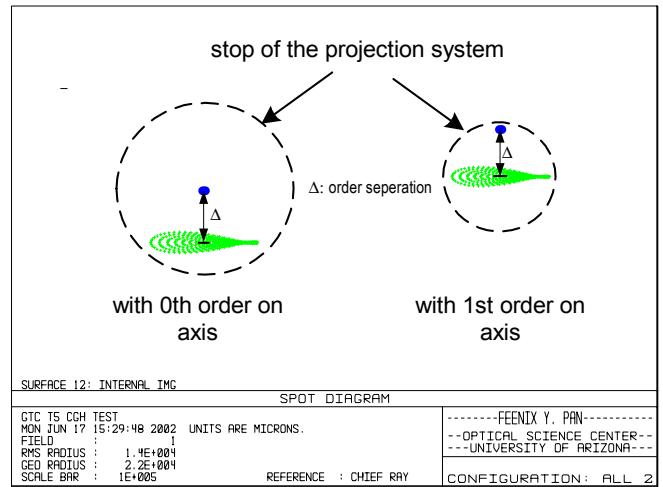


Figure 5-5: Locating 1st order on-axis reduces projection system stop size

5.3 Making the test cost effective and less complex

Utilizing conclusions reached in the previous two sections can reduce the test cost and simplify the system design. With a simple co-axial setup, the surface slope of the test plate can be reduced nearly three orders of magnitude, thus significantly reduce the cost of the test. Locating the aberrated 1st CGH diffraction order to the axis of the projection system reduces the stop size of the projection system by ~20%. This reduction of stop size simplifies the design of the projection system considerably since the complexity of the projection system has a cubic dependency on the stop size.

CONCLUSION

This report accomplishes two tasks. It first presents the successful experimental validation on the new proposed method of measuring off-axis aspherical segments using CGH and a test plate. This is followed by a detail tolerance analysis on the experimental setup. From the tolerance analysis, two important conclusions were drawn on how to make the test more cost effective and less complex.

This study shows that this new method is optimal for measuring segments of aspheric primary mirrors, but it can also be applied to any aspheric surface, convex or concave. For mirror segments that will be phased together, this ensures that all segments will form a single, continuous surface when they are assembled. To summarize, this new method is: 1) accurate, 2) cost effective, 3) easy to implemented and 4) ideal for providing excellent relative radius matching and accurate axis location.